Chemical Engineering Journal 264 (2015) 197–210

Contents lists available at ScienceDirect

Chemical Engineering Journal

journal homepage: www.elsevier.com/locate/cej

Acetaldehyde and acetic acid adsorption on TiO_2 under dry and humid conditions

F. Batault [a,b,c], F. Thevenet [a,b,*], V. Hequet [c], C. Rillard [c], L. Le Coq [c], N. Locoge [a,b]

[a] Université Lille Nord de France, F-59000 Lille, France
[b] Mines Douai, SAGE, F-59508 Douai, France
[c] GEPEA, UMR CNRS 6144, Mines Nantes, DSEE, 4 rue Kastler, BP 20722, 44307 Nantes Cedex 3, France

HIGHLIGHTS

- Quantitative determination of VOC adsorption parameters on TiO_2.
- Proposition of competitive adsorption model for polar VOC and H_2O co-adsorption.
- Determination of model VOC adsorption pathways on TiO_2.
- Use of single VOC adsorption parameters to understand multi-VOC adsorption.

GRAPHICAL ABSTRACT

Layout of ① acetaldehyde and ② subsequent acetic acid and acetaldehyde co-adsorption on P25 TiO_2 under 50% relative humidity and 23 °C.

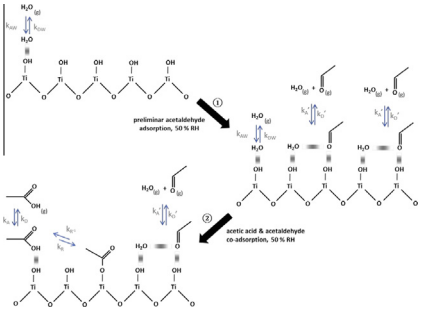

ARTICLE INFO

Article history:
Received 22 August 2014
Received in revised form 21 October 2014
Accepted 26 October 2014
Available online 3 November 2014

Keywords:
Adsorption
TiO_2
Acetaldehyde
Acetic acid
Relative humidity

ABSTRACT

Adsorption plays a key role in the volatile organic compound (VOC) photocatalytic oxidation performance and kinetic behavior. It can lead to VOC mixture sequential treatment or even photocatalyst deactivation. The aim of this work is to determine qualitative and quantitative data regarding VOC adsorption on P25 TiO_2. Acetaldehyde and acetic acid adsorption on TiO_2 have been studied under both dry and humid conditions. Three experimental methods have been used: breakthrough curves, room temperature desorptions and temperature-programmed desorptions. First, acetaldehyde and acetic acid adsorptions are studied individually. Dry and humid experiments provide complementary pieces of information to identify the adsorption modes, in accordance with literature. The Langmuir model parameters (adsorption constant (K), reversible and irreversible maximum adsorbed amounts ($q_{m,rev}$ and $q_{m,irr}$), and adsorption enthalpy ΔH) are determined for each VOC. Based on experimental results, a model for acetaldehyde and water co-adsorption is proposed, taking into account the specific interaction between acetaldehyde and water molecule. Regarding acetic acid, a reactive adsorption pathway is proposed and a kinetic model is developed to describe the reactive adsorption. Finally, in order to understand multi-VOC interaction on TiO_2 surface, the sequential adsorption of acetaldehyde and acetic acid is investigated and confronted with the single-VOC data. As a result, single VOC adsorption parameters are useful to understand and predict multi-VOC photocatalytic oxidation.

* Corresponding author at: Mines Douai, Dpt SAGE, F-59500 Douai, France.
E-mail address: frederic.thevenet@mines-douai.fr (F. Thevenet).

http://dx.doi.org/10.1016/j.cej.2014.10.089
1385-8947/

1. Introduction

Indoor air quality is nowadays a concerning public health issue. Part of the indoor air pollution is related to Volatile Organic Compounds (VOCs) [1]. Advanced oxidation processes – such as non-thermal plasma [2] or photocatalytic oxidation (PCO) [3–5] – are promising techniques to remove VOCs from indoor air. Among these technologies, photocatalytic oxidation shows an increasing interest, as evidenced by the number of academic research articles and by the number of patents for indoor air treatment photocatalytic oxidation [6].

Photocatalytic VOC oxidation is a heterogeneous process, meaning that VOC adsorption on the photocatalyst surface is a key step to initiate the reaction. The role of adsorption is particularly critical in the case of VOC mixture treatments. Indeed, individual photocatalytic VOC removal rates tend to decrease in the presence of other VOCs, as reported in literature [7–9]. The hypothesis generally raised to explain this phenomenon is the competitive adsorption of VOCs on the photocatalyst surface. For instance, Chen et al. [7] compared the degradation rates of five VOCs in single-VOC condition and in several VOC mixtures. All the tested VOCs evidenced a significant rate decrease while being treated in a 16-VOC mixture. The impacting VOCs are not only primary pollutants, but may be part of the intermediates produced during the photocatalytic reaction itself [9,10]. Indeed, Zorn et al. [9] evidenced the competitive role of intermediates. They performed propanone photocatalytic oxidation. During this degradation, they injected some ethanol. Some acetaldehyde formed by ethanol oxidation and was then degraded. The propanone rate was severely decreased when ethanol was present in gas-phase, but also when acetaldehyde was still present and ethanol was completely eliminated from gas-phase.

As a consequence, data about VOC adsorption onto photocatalysts are needed for a better understanding of the VOC photocatalytic treatment kinetic and to predict the behavior of a VOC mixture submitted to a photocatalytic treatment. Former articles dealing with VOC adsorption on TiO_2 originate from two distinct research fields: surface science and catalysis. Surface science studies generally focus on adsorption modes, but rarely provide quantitative data which can be used for photocatalytic oxidation kinetic considerations. On the contrary, in the field of catalysis, studies generally determine global Langmuir adsorption constants without any adsorption mode consideration. These parameters are obtained from adsorption experiments [11–13] or from photocatalytic oxidation kinetic studies [14–19]. Some photocatalytic oxidation works [10,20] use adsorption modes to get a better understanding of their reaction kinetics.

This work aims at determining quantitative adsorption data based on adsorption mode considerations, which could be efficiently used for photocatalytic reaction understanding and modeling. For this purpose, the VOC adsorption modes will be investigated, to know whether VOCs compete for the same TiO_2 adsorption sites or not. For each mode, the Langmuir model maximum adsorbed amount q_m [μmol m^{-2}] and adsorption constant K [$ppmv^{-1}$] will be determined. Binary VOC adsorption will then be investigated to assess if the obtained single-VOC adsorption data enable to understand multi-VOC adsorption. Please note that all the used symbols are described in Table 1.

The VOCs selected for this study are acetic acid and acetaldehyde. Both VOCs are indoor air primary pollutants [1,21]. Moreover, acetaldehyde is a crucial intermediate in VOC photocatalytic oxidation. Indeed, acetaldehyde and formaldehyde are known to be the most concentrated intermediates in toluene

Table 1
Nomenclature of used notations.

Parameter	Description	Unit
C	VOC gas phase concentration	ppmv
C_W	Water concentration	$\%RH^{-1}$
h	Plank constant	J s
k	Boltzmann constant	$J\ K^{-1}$
k_A	VOC adsorption kinetic constant	$ppmv^{-1}\ s^{-1}$
k_{AW}	Water adsorption kinetic constant	$\%RH^{-1}\ s^{-1}$
k'_A	Cluster adsorption kinetic constant	$ppmv^{-1}\ \%RH^{-1}\ s^{-1}$
k_D	VOC desorption kinetic constant	s^{-1}
k_{DW}	Water desorption kinetic constant	s^{-1}
k_D'	cluster desorption kinetic constant	s^{-1}
k_R	Acetic acid – acetate group reaction kinetic constant	$\mu mol^{-1}\ m^2\ s^{-1}$
$k_{R\text{-}1}$	Acetate group – acetic acid reaction kinetic constant	$s^{-1}\ m^2\ s^{-1}$
K	adsorption constant	$ppmv^{-1}$
K_H	Apparent adsorption constant	$ppmv^{-1}$
K'	Cluster adsorption constant	$ppmv^{-1}\ \%RH^{-1}$
n	Water/VOC molar ratio in clusters	–
q	VOC adsorbed quantity	μmol m^{-2}
q_{CLU}	Cluster adsorbed quantity	μmol m^{-2}
q_C	Non desorbed quantity during TPD	μmol m^{-2}
q_{expe}	VOC experimentally calculated adsorbed quantity	μmol m^{-2}
q_{irr}	VOC irreversibly adsorbed quantity	μmol m^{-2}
q_{OH}	Free –OH group quantity	μmol m^{-2}
q_m	VOC monolayer adsorbed quantity	μmol m^{-2}
$q_{m\ irr}$	VOC monolayer irreversibly adsorbed quantity	μmol m^{-2}
$q_{m\ OH}$	Total –OH group quantity	μmol m^{-2}
$q_{m\ rev}$	VOC monolayer reversibly adsorbed quantity	μmol m^{-2}
q_{rev}	VOC reversibly adsorbed quantity	μmol m^{-2}
q_{sim}	VOC simulated adsorbed quantity	μmol m^{-2}
q_W	Water adsorbed quantity	μmol m^{-2}
R	Perfect gases constant	$J\ mol^{-1}\ K^{-1}$
T	Temperature	K
α	Acetate group – acetic acid reaction constant	–
ΔH	VOC adsorption enthalpy	$kJ\ mol^{-1}$
ΔH_0	VOC adsorption enthalpy at zero coverage	$kJ\ mol^{-1}$
ΔH_1	VOC adsorption enthalpy at full coverage	$kJ\ mol^{-1}$
ϑ	Coverage rate	–

[22], decane [23] and other VOCs [24] PCO. Acetic acid is an oxidized form of acetaldehyde; it is thus likely to exist in adsorbed phase during a photocatalytic reaction involving acetaldehyde. The photocatalyst selected in this work is P25-Degussa titanium dioxide (TiO_2). The targeted adsorption conditions were room temperature (23 ± 1 °C) and 50% relative humidity, which are close to realistic indoor air conditions [25]. Nevertheless, for a better understanding of the surface phenomena, adsorption was first studied in dry condition. Humidity influence was investigated in a second set of experiments. The adsorptions of both VOCs are first studied separately to distinguish their specific behaviors. Then, the adsorption of mixture is carried out to evaluate if the data obtained for single-VOC adsorption can be transposed to multi-VOC adsorption and used to interpret the competitive adsorption phenomena.

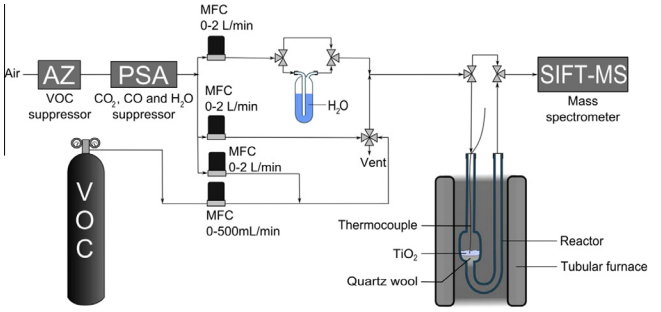

Fig. 1. General scheme of the experimental setup. MFC, mass flow controllers; AZ, zero air generator; PSA, pressure swing adsorption air purifier; VOC, volatile organic compound; SIFT MS, selected ion flow tube mass spectrometer.

2. Experimental

2.1. Materials

Commercially available P-25 Degussa TiO_2 powder is used. This material is purchased from Aeroxide. In order to avoid any critical pressure drop caused by the free powder compaction along experiments, TiO_2 powder has been processed as follow: it is first pressed to obtain a 1 mm thick disc. This disc is then crumbled and sieved to get the targeted 200–500 μm pellets. Before each experimental sequence, the TiO_2 bed is heated to 400 °C to remove undesired species from the surface, without impacting the material morphology and to ensure a reproducible surface state. The obtained TiO_2 specific surface is measured using a nitrogen adsorption BET setup. The determined value is 57 ± 3 m^2/g, which is coherent with the supplier specifications (50 ± 15 m^2/g).

In this work, gas concentrations are all given as volume mixing ratio in parts per million (ppmv), parts per billion (ppbv) or parts per trillion (pptv). Acetic acid (106 ± 2 ppmv in nitrogen) and acetaldehyde (518 ± 10 ppmv in nitrogen) certified cylinders are supplied by Praxair. Nitrogen (Air Liquide Alphagaz-2) cylinders are used during high-temperature experiments. They contain less than 0.5 ppmv H_2O, 0.1 ppmv O_2, 0.1 ppmv CO_2 and 0.1 ppmv VOCs. Treated air is used as diluting gas during room temperature experiments. It is produced by catalytic zero air generator (Claind 2020) coupled with a Pressure Swing Adsorption (PSA) device (Parker Balston 75-52). This treated air is called "zero air". The residual concentrations in zero air are: VOCs < 100 pptv, CO_2 < 10 ppbv and H_2O < 2 ppmv.

2.2. Experimental setup

The general experimental setup is presented on Fig. 1. The inlet flow is prepared by gas dilution. Mass Flow Controllers (MKS instruments) are used to set the VOC concentration and relative humidity. Calibrated VOC Cylinders provided by Praxair are diluted with nitrogen or zero air. The gas flow relative humidity is set by sending dilution gas through a deionized water bubbler maintained at room temperature. For the desorption experiments, the reactor is purged with the dilution gas without any VOC. A 4-way valve enables a rapid switch between the two gas streams: the pure dilution gas and the VOC/dilution gas mixture.

Experiments are carried out in a fix-bed flow reactor. This quartz-made reactor includes a bulb and U-shaped tubing. The tubing inner and outer diameters are respectively 4 and 6 mm. The bulb inner diameter is 15 mm and its length is 30 mm. The sorbent bed is placed in the bulb bottom. The typical TiO_2 mass used for experiments is 80 mg, depending on the sorption ability of the investigated VOC. A quartz wool plug is used to maintain the TiO_2 bed in the reactor. The reactor and the sorbent bed are depicted in Fig. 1.

The reactor can be by-passed using two three-way valves and a pipe. During thermal pretreatment and thermal desorptions, the reactor is heated with a tubular furnace (Nabertherm P330) with a heating rate of 10–40 K/min, up to 673 K. The sorbent temperature is continuously monitored using a K-type thermocouple located inside the reactor. Its tip is located in the center of the sorbent bed. The gas stream relative humidity is monitored with a Testo probe (±1% accuracy), to make sure the sorbent is subjected to the targeted relative humidity condition.

At the reactor outlet, VOC concentrations are monitored with a Selected Ion Flow-Tube (SIFT) mass spectrometer (Syft Voice 200). SIFT mass spectrometry is based on analytes chemical ionization. This technology generates three precursor ions: H_3O^+, NO^+ and O_2^+. Precursor ions are sequentially selected by a first quadripole. Then, they react with the analytes in a flow tube to produce ionized molecules, which are separated by a second quadripole and counted. This device enables the calculation of analyte theoretical concentrations using: the kinetic of ionization reactions in the flow tube, the ionized molecule and remaining precursor quantities, and the residence time inside the flow tube. This calculation is based on theoretical data, and can be affected by the operating conditions. For more reliable concentration measurements, this mass spectrometer is experimentally calibrated regularly, using the dilution bench and VOC cylinders.

In this work, acetaldehyde concentration is monitored using m/z = 45 a.m.u (H^+ association with acetaldehyde) during H_3O^+ ionization phase and with m/z = 43 a.m.u (hydride abstraction from acetaldehyde) during NO^+ ionization phase. Acetic acid concentration is monitored using m/z = 61 a.m.u (H^+ association with acetic acid) during H_3O^+ ionization phase and with m/z = 90 a.m.u (NO^+ association with acetaldehyde) during NO^+ ionization phase. The limits of detection are 49 ppb for acetaldehyde and 100 ppb for acetic acid, for a one-minute integration time.

2.3. Experimental procedures and data treatments

Three complementary methods are used to characterize VOC adsorption on TiO_2:

(i) breakthrough curves,
(ii) room temperature desorption (flushing),
(iii) temperature-programmed desorption.

In order to illustrate these techniques and to evidence which parameter are accessible using these techniques, the theoretical plots of outlet concentration and adsorbed quantity as a function of time are reported in Fig. 2.

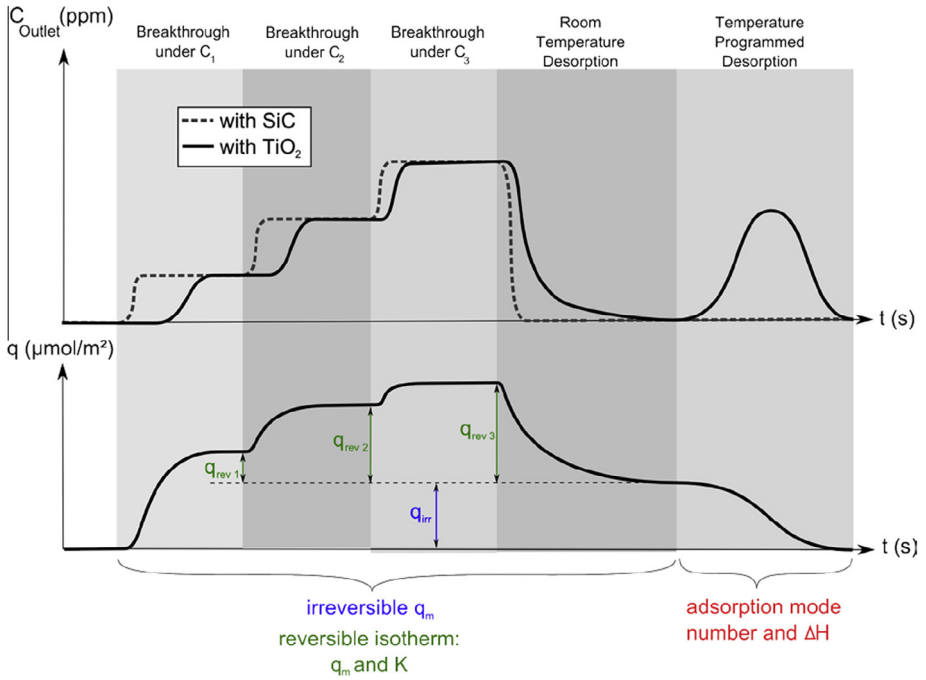

Fig. 2. Theoretical plots of (i) breakthrough curve, (ii) room temperature desorption (RTD) and (iii) temperature-programmed desorption (TPD), showing the reactor outlet VOC concentration, the calculated adsorbed quantity and the obtained quantitative and qualitative data along the different experimental steps.

First, these methods provide qualitative information on adsorption modes: number of adsorption modes and correspondence with reversibly or irreversibly adsorbed fractions. Obtained information is completed with the ones from literature about the nature adsorption sites and the nature of the VOC-surface bounds.

Second, experimental results also provide quantitative information: the adsorbed quantities versus the concentration, so-called the adsorption isotherms. Determined isotherms have been fitted using the Langmuir model [26] (Eq. (1)) to extract two adsorption parameters: the maximum adsorbed quantity (q_m) and the adsorption constant (K). This model gives the adsorbed quantity versus the gas-phase concentration at equilibrium state for one adsorption mode. It is valid in the presence of low concentrations, which lead to less than a monolayer of adsorbed VOCs on the surface. For this reason, the adsorbed quantity can be written as a coverage rate: ϑ. The ϑ parameter is defined as the ratio between the adsorbed quantity and the maximum adsorbed quantity for a monolayer.

$$q = q_m \cdot \vartheta = q_m \frac{KC}{1 + KC} \quad (1)$$

In Eq. (1), the adsorbed quantity and the gas-phase concentration are respectively depicted by q (µmol/m^2) and C (ppmv). This model involves two parameters: the maximal adsorbed quantity q_m (µmol/m^2) and the adsorption constant K (ppmv^{-1}). Adsorption constant depends on the VOC-surface interaction, which can be quantified by the adsorption enthalpy ΔH (kJ/mol). Eq. (2) gives the relation between K and ΔH, based on statistical physics calculations [27].

$$K = \frac{h^3}{kT(2\pi mkT)^{\frac{3}{2}}} e^{-\frac{\Delta H}{RT}} \quad (2)$$

In Eq. (2), h (J s) is the Planck constant, k (J K^{-1}) is the Boltzmann constant, R (J K^{-1} mol^{-1}) is the perfect gases constant, m (kg) is the VOC molecular mass and T (K) is the temperature. The adsorption constant is calculated in Pa^{-1} and can be converted into ppmv^{-1}.

Since the presence of molecules, which are already adsorbed on the surface, can affect the VOC-surface interactions, K and ΔH can vary with the coverage rate: ϑ. In that case, it may be necessary to describe the variation of these parameters with ϑ, or at least to indicate their respective values when ϑ is close to 0 (low coverage) or close to 1 (high coverage).

2.3.1. Breakthrough curves

Breakthrough curves make possible the determination of the adsorbed VOC quantity on TiO_2 at equilibrium for a gas phase composition. These quantities are used to plot the isotherm curve, i.e., the adsorbed quantity versus the concentration. The sorbent is submitted to a VOC concentration step. The outlet VOC concentration curve is recorded twice: (i) when TiO_2 (the sorbent) is placed in the reactor, and (ii) when silicon carbide (SiC) which does not adsorb the VOC, is place instead of TiO_2 (Fig. 2). These curves are used to calculate the quantity of VOC adsorbed on TiO_2 using a reactor mass balance: the adsorbed quantity is calculated by integrating the difference between both TiO_2 and SiC outlet VOC concentration curves. In order to obtain several 'adsorbed quantity'/'concentration' couples within only one experiment, "multiple breakthrough" curves have been carried out. To perform a multiple breakthrough, the inlet flow VOC concentration describes several increasing steps. The time between each concentration increment is kept long enough to reach the equilibrium. The equilibrium is known to be reached when the outlet concentration remains constant and corresponds to the input concentration. Multiple breakthroughs have been performed with various first step concentrations to make sure that the data obtained from a first step and from the other steps are comparable. All breakthrough curves are determined at 23 ± 1 °C.

2.3.2. Room temperature desorption (RTD)

A room temperature desorption (RTD) is operated after each breakthrough curve. Once the last adsorption equilibrium of the multiple-breakthrough curve has been reached, the four-way valve

is switched to expose the sorbent to a zero air flow containing the same relative humidity than the adsorption carrier gas. Similarly to breakthrough curves, this experimental step is performed at 23 ± 1 °C. Part of the VOC adsorbed along breakthrough may desorb during this step (Fig. 2).

Similarly to breakthrough, the desorbed quantity is calculated by integrating the difference between the outlet concentration curves obtained (i) with the TiO_2 bed and (ii) with the SiC beds. This desorbed amount is attributed to the reversibly adsorbed fraction of the VOC. The remaining adsorbed quantity can be attributed to the irreversibly adsorbed fraction. Reversibly and irreversibly fractions do not necessarily correspond to two different adsorption modes. Indeed, these fractions can contain more than one adsorption mode, since a VOC can have more than two adsorption modes. Moreover, one adsorption mode can split into reversible and irreversible fractions, due to transient kinetic phenomena [28]. Regarding the adsorption mode identification, complementary pieces of information are used from literature and from the temperature-programmed desorptions.

2.3.3. Temperature-programmed desorption (TPD)

After the RTD, according to the temperature-programmed desorption (TPD) method [29,30], the reactor is exposed to a nitrogen flow and submitted to a 15 ± 1 K/min heating ramp to induce the desorption of the irreversibly adsorbed fraction. The sorbent temperature and the outlet VOC concentration are measured and recorded, and can be plotted as reported on Fig. 2. TPD have been carried out only in dry condition, because the surface hydration and hydroxylation cannot be controlled along heating.

The TPD curve can be modeled to estimate the adsorption mode enthalpies. Under our experimental conditions, desorption is assumed to be under quasi-equilibrium. This assumption is supported by the work of Kanervo et al. [31]. These authors performed TPD curve modeling for a reactor equivalent to the one used in that work and for similar experimental conditions. They evidenced that the quasi-equilibrium hypothesis is a good approximation of the complete adsorption–desorption model. Thus, the equilibrium Langmuir model (Eq. (1)) is used. The desorbed quantity along the TPD is calculated first using the TPD VOC concentration curve and a reactor mass balance. The desorbed quantity curve is subtracted from the irreversible fraction to obtain the experimental adsorbed quantity (denoted by q_{expe}) curve. Then, the simulated adsorbed quantity (denoted by q_{sim}) curve is calculated with measured temperatures and concentrations, and using the experimental quantity for the coverage calculation. A multi-site equation is used. The number of modes is chosen according to the number of observed peaks on the concentration TPD curve. For example, Eq. (3) is the relation used for two modes (denoted A and B). Adsorption constants are calculated as functions of temperature and coverage rate (ϑ). For the mode "i", the zero and full coverage enthalpies are respectively denoted by ΔH_{i0} and ΔH_{i1}. The coverage rate ϑ_i is calculated as the ratio of the remaining adsorbed quantity of the concerned mode and its q_{mi} value (Eq. (5)). A constant quantity (denoted by q_C) was added to take in account that the experimental adsorbed quantity do not reach zero, due to desorption as other molecules. q_m and ΔH were then adjusted to make the q_{sim} function fit the q_{expe} curve, using an optimization algorithm.

$$q_{sim}(t) = q_{mA}\frac{K_A(t).C}{1+K_A(t).C} + q_{mB}\frac{K_B(t).C}{1+K_B(t).C} + q_C \quad (3)$$

$$K_i(t) = \frac{h^3}{k.T(t)[2\pi.m.k.T(t)]^{\frac{3}{2}}} e^{-\frac{\Delta H_{i0}+\vartheta_i(t).[\Delta H_{i1}-\Delta H_{i0}]}{R.T(t)}} \quad (4)$$

$$\vartheta_A(t) = \frac{q_{expe}(t) - q_{mB} - q_C}{q_{mA}} \quad (5)$$

3. Results and discussion

3.1. Acetaldehyde adsorption in dry and humid conditions

Adsorption on TiO_2 was studied first for acetaldehyde, without competition with any other VOC. Acetaldehyde adsorption is first studied in dry condition, since the adsorption qualitative and quantitative features could be influenced by water co-adsorption. In a second set of experiments, the impact of water is investigated in the presence of 50% relative humidity.

3.1.1. Acetaldehyde adsorption in dry condition: reversibly and irreversibly adsorbed fractions

Multiple breakthrough curves and Room Temperature Desorptions (RTD) of acetaldehyde on TiO_2 have been performed in the 20–520 ppmv concentration range. These experiments make possible the calculation of the adsorbed quantities under different concentrations and the remaining adsorbed quantity after zero air exposure. Fig. 3 shows one of these experimental multiple breakthrough curves. In the case of Fig. 3, TiO_2 has been successively submitted to 62 ppmv, 82 ppmv and 97 ppmv acetaldehyde concentrations to reach the corresponding adsorption equilibriums. Then, it is submitted to a zero air flushing to desorb the reversibly adsorbed fraction corresponding to the third adsorption equilibrium. The total adsorbed quantity reaches 17.5 μmol/m^2 during the first concentration step. During the following adsorption steps, it only increases by 0.08 and 0.06 μmol/m^2. During the RTD, the total adsorbed amount decreases by 0.68 μmol/m^2 leading to a remaining adsorbed amount of 16.9 μmol/m^2. It can first be noticed that only a small part of the adsorbed acetaldehyde desorbs during the RTD. Most of acetaldehyde adsorption in dry condition is irreversible: the reversibly adsorbed fraction is only 4% of the total adsorbed quantity at the third step. It can also be noticed that the quantity adsorbed during the first step is huge, relatively to the quantities adsorbed during the second and the third steps. Multiple breakthrough and RTD sequences have been performed 8 times with different step numbers and different first-step concentrations. Every time, the first step adsorbed quantity represents more than 97% of the last-step total adsorbed amount. It means that the irreversibly adsorbed fraction is mainly adsorbed during

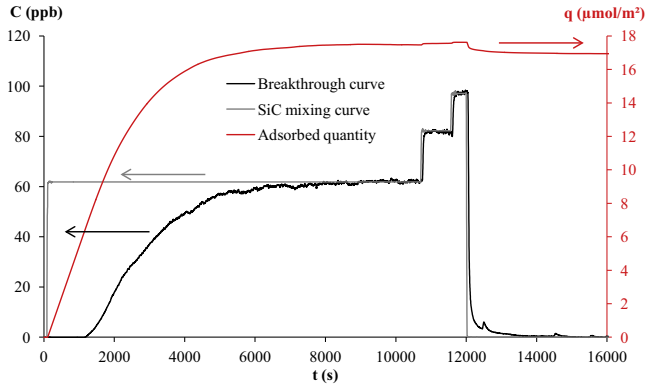

Fig. 3. Multiple breakthrough and room temperature desorption (RTD) sequence typical curves for acetaldehyde experiments in dry air: Breakthrough curve on TiO_2 (black line) and SiC mixing curve (grey line) outlet concentrations and calculated adsorbed quantity (red line) versus time. (For interpretation of the references to colour in this figure legend, the reader is referred to the web version of this article.)

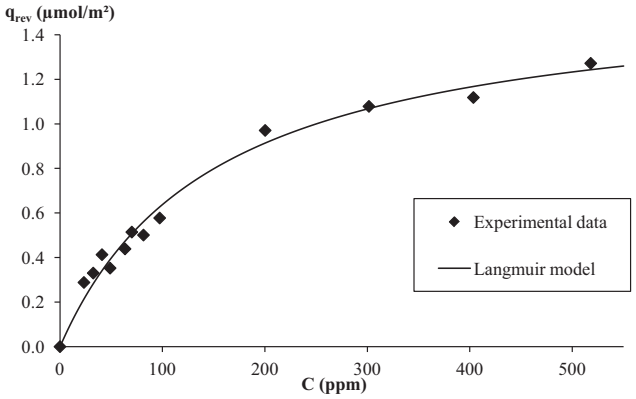

Fig. 4. Acetaldehyde reversibly adsorbed fraction isotherm on P25 TiO_2 under dry condition, at 23 ± 1 °C.

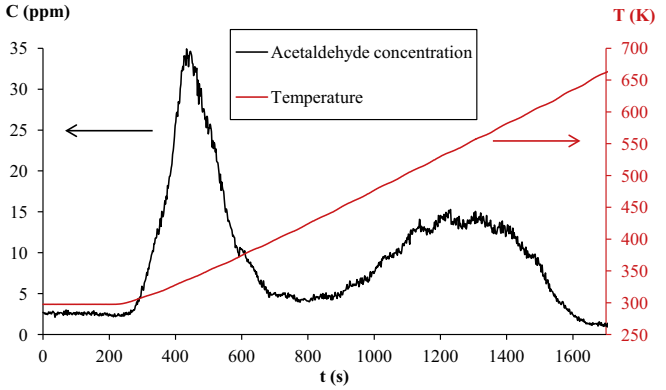

Fig. 5. Temporal profile of acetaldehyde desorbed along the temperature-programmed desorption (TPD) on P25 TiO_2, under 100 mL/min dry N_2 flow and 16 K/min heating.

the first step of each experimental sequence. The irreversibly adsorbed amount calculated for the last step can thus be used to calculate the reversibly adsorbed quantity of every step for each experimental sequence, as shown on Fig. 2.

Based on the 8 multiple breakthrough sequences, reversibly and irreversibly adsorbed quantities have been determined for various concentrations of acetaldehyde ranging from 20 to 520 ppmv. The eight values of the irreversibly adsorbed fraction have been obtained and averaged. Standard deviation has been calculated to determine the uncertainty associated to the irreversibly adsorbed amount. The obtained value is 14.6 ± 4.8 µmol/m^2.

The reversibly adsorbed quantities increase with the VOC concentration. Then, they have been plotted as a function of acetaldehyde gas-phase concentration (Fig. 4). Each point is the average of three experimental values. This curve has been fitted with the Langmuir model in order to determine the adsorption parameters ($q_{m,rev}$ and K) of the reversibly adsorbed mode. Parameters obtained from this set of experiment are $q_{m,rev}$ = 1.61 ± 0.22 µmol/m^2 and $K = 6.6.10^{-3} \pm 1.2 \times 10^{-3}$ ppmv^{-1}. The $q_{m,rev}$ value of the reversibly adsorbed fraction is one order of magnitude lower than the irreversibly adsorbed fraction one. This difference will be discussed further with adsorption mode considerations.

3.1.2. Acetaldehyde adsorption in dry condition: adsorption modes

The adsorption modes corresponding to the observed reversible and irreversible fractions were investigated with the temperature-programmed desorption (TPD) method, and compared with available literature data. Following the multiple breakthrough curve and RTD experimental sequences, TPDs have been conducted to characterize the adsorption modes from the irreversibly adsorbed part. Fig. 5 shows the outlet concentration curve obtained during one of these TPD. TPD are performed under a 100 mL/min nitrogen flow, with a 15.6 K/min heating rate.

The TPD curve shows two distinct peaks, corresponding to two adsorption modes. Among the remaining adsorbed quantity after the RTD, only 2% desorbed as acetaldehyde during the TPD. Most of the irreversibly adsorbed acetaldehyde molecules are not released as acetaldehyde during the TPD. Ethanol, acetic acid, 2-butenal (crotonaldehyde), benzene, carbon monoxide and carbon dioxide have been detected at the reactor outlet during the TPD. The difference between the irreversibly adsorbed quantity and the quantity desorbed as acetaldehyde during the TPD can be correlated to the adsorption modes of acetaldehyde on TiO_2. Acetaldehyde adsorption modes onto TiO_2 are described in literature. Acetaldehyde adsorption on TiO_2 occurs as two modes. Acetaldehyde adsorbs first molecularly as a poorly stable mode by H-bond onto −OH sites and as a more stable mode through a chemical bond between the acetaldehyde oxygen and the TiO_2 surface Lewis acid sites [32,33]. Part of the weakly and strongly adsorbed acetaldehydes molecules then condensates into 3-hydroxybutanal by β-aldolization [32], which dehydrates into 2-butenal [32,33]. The relative quantities of strongly adsorbed acetaldehyde, 3-hydroxybutanal and 2-butenal depend on the temperature and on other surface conditions. Some authors reported that only 2-butenal exists at room temperature [32]. In other works, part of acetaldehyde is converted into 2-butenal during both acetaldehyde adsorption and surface flushing [34]. It was also evidenced that acetaldehyde can adsorb as dimers, which both impede the condensation and release one of the acetaldehyde monomers while flushing [35]. Oxidation and reduction reactions can also occur on chemically-bonded acetaldehyde, leading to adsorbed acetate and ethoxy groups [33]. While heating the surface above 400 K, benzene is produced from acetaldehyde and 2-butenal [33].

These literature data enable to explain the TPD curve and the presence of the other detected gases. The first peak noticed on Fig. 5 can be attributed to the H-bonded adsorption mode. It can be noticed that this peak is already observed close to room temperature. Thus, this weakly bonded mode could be in some extent considered as the continuation of the RTD. The reversibly adsorbed fraction can thus be assigned to the H-bonded mode.

The second desorption peak (Fig. 5) could be attributed to the chemically-bonded acetaldehyde molecules. The irreversibly adsorbed quantity which did not desorb as acetaldehyde during the TPD corresponds to (i) 2-butenal, ethoxy groups and acetate groups formed during the adsorption and the RTD, which respectively desorb as 2-butenal, ethanol and acetic acid during the TPD, and (ii) the thermal conversion of acetaldehyde and 2-butenal into benzene and of the other adsorbed species into CO and CO_2. In this work and regarding the targeted applications, the chemically-bonded acetaldehyde and the 2-butenal molecules can be considered as one apparent mode, since both are strongly-bonded and irreversibly-adsorbed modes.

The significant quantitative difference between both modes could be related to the surface pretreatment under dry air. Indeed, the small fraction of reversibly adsorbed acetaldehyde is due to the low hydroxyl group surface density. When the surface is pretreated at 400 °C, Nagao et al. [36] evidenced that the hydroxylation rate dramatically decreases. The number of hydroxyl groups per nm^2 falls from 7.88 (13.1 µmol/m^2) for a 25 °C evacuation, to 0.132 (0.219 µmol/m^2) for a 600 °C pretreatment. This consideration support a very low reversibly adsorbed amount compared to the irreversibly adsorbed fraction which is not impacted.

ΔH and $q_{m,rev}$ related to the weakly bonded adsorption mode are determined from TPD curve, using the method described in Section 2.3.3. The remaining adsorbed quantity curve is fitted using the measured temperature and concentration curves (Fig. 5). In order to compare values obtained from reversible isotherm and from TPD, both set of data are presented in Table 2. Obtained values do not show any significant differences. This result confirms that the reversible adsorption and the first TPD peak correspond to the same adsorption mode.

3.1.3. Acetaldehyde adsorption in humid air

To assess the influence of humidity on acetaldehyde adsorption on TiO_2, breakthrough and RTD of acetaldehyde have been performed under 50% relative humidity. In this condition, the adsorption has been found to be totally reversible. Water adsorption on TiO_2 is reported [37] to occur as (i) dissociative adsorption, which increases the hydroxyl site density on TiO_2 surface and (ii) physical adsorption of an H-bonded water molecules ad-layer. Both phenomena increase with relative humidity. Hydroxylation has been reported [10] to be complete above a RH threshold below 10%. Water molecular adsorption is described in literature [10] to be in accordance with the BET model, and to reach a complete monolayer coverage for relative humidities higher than 57%. The total surface hydroxylation could be an explanation to the absence of irreversible adsorption under 50% RH. A similar behavior has been reported [37] for methanol adsorption on anatase as methoxy groups, which only occurs below 10 Torr water vapor pressure. It can be noticed that at 296 K, 50% relative humidity corresponds to 10.5 Torr. Other authors found a lower threshold for water monolayer physisorption. For example, Sivachandiran et al. [38] notice a changing in isopropyl alcohol adsorption on P25 TiO_2 around 30% relative humidity. To resume, these works tend to show that the total surface hydroxylation prevents acetaldehyde to adsorb irreversibly.

At 50% RH, acetaldehyde adsorption on TiO_2 only occurs as reversible physical adsorption. The adsorbed quantities obtained from the breakthrough curves makes possible the plotting of adsorption isotherm for the reversibly adsorbed fraction (Fig. 6). This curve has been fitted with a Langmuir model to compare the adsorption parameters of acetaldehyde physical adsorption mode under dry and humid conditions. They are reported in Table 3.

The influence of water on acetaldehyde physical adsorption onto TiO_2 hydroxyl groups can be figured out with a Langmuir acetaldehyde–water competitive adsorption model. This model can be written as reported in Eq. (6).

$$q_{rev} = q_{m,rev}\frac{KC}{1 + KC + K_W C_W} \quad (6)$$

In Eq. (6), q_{rev} (μmol/m^2) is the amount of physically adsorbed acetaldehyde, $q_{m,rev}$ (μmol/m^2) is the maximum adsorbed quantity, K (ppmv^{-1}) is the acetaldehyde adsorption constant, C (ppmv) is the acetaldehyde gas-phase concentration, K_W (ppmv^{-1}) is the water ad-layer molecules adsorption constant and C_W (ppmv) the water gas phase concentration. For a given water concentration, this equation can be rewritten as an apparent Langmuir pattern in Eq. (7).

Table 2
Langmuir model parameters of acetaldehyde reversibly adsorbed fraction on P25 TiO_2, under dry condition.

Experimental procedure	$q_{m,rev}$ (μmol/m^2)	K (ppmv^{-1})	ΔH (kJ/mol)
Reversible isotherm	1.61 ± 0.22	0.0066 ± 0.0012	−61.6 ± 0.5
TPD	1.63 ± 0.17	Ø	−65.3 ± 6.6

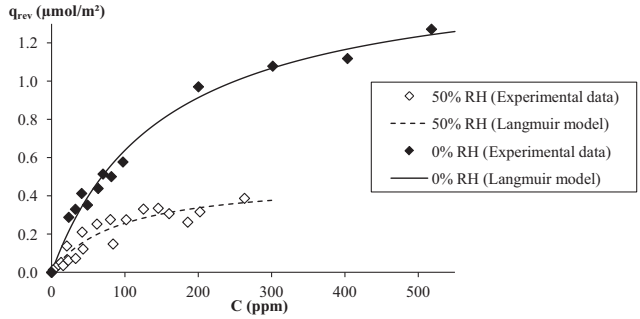

Fig. 6. Acetaldehyde reversible adsorption on P25 TiO_2 isotherm under dry and humid condition, at 23 °C.

Table 3
Langmuir model constants for the reversibly adsorbed fraction of acetaldehyde on P25 TiO_2 under dry and humid condition and 23 °C, calculated with the corresponding isotherms (Fig. 6).

Relative humidity (%)	$q_{m,rev}$ (μmol/m^2)	K (ppmv^{-1})
0	1.61 ± 0.22	0.0066 ± 0.0012
50	0.49 ± 0.14	0.0109 ± 0.0040

$$q = q_{m,rev}\frac{K_H C}{1 + K_H C} \quad (7)$$

In Eq. (7), the maximum adsorbed quantity is not affected by the water ad-layer presence, and the pseudo adsorption constant K_H (ppmv^{-1}) is expected to be lower than the dry adsorption constant, depending on the water vapor concentration, as shown in Eq. (8).

$$K_H = \frac{K}{1 + K_W C_W} \quad (8)$$

Thus this model predicts that the $q_{m,rev}$ value should not be effected by the adsorption competition. Since the surface is more hydroxylated at 50% RH than in dry atmosphere, the $q_{m,rev}$ value is expected to be higher in humid condition. The model also predicts that the pseudo adsorption constant should be lower in humid condition than in dry one.

As reported in Table 3, the value of $q_{m,rev}$ is higher in dry condition than in humid one, in spite of the fact that there are more hydroxyl groups in humid condition than in dry one. For VOC physisorption on TiO_2 hydroxyl groups, the $q_{m,rev}$ value depends on the surface of the adsorbed molecule and on the number of available hydroxyl sites [36]. Then, the decrease of the reversible fraction $q_{m,rev}$ can be explained by two hypotheses: (i) part of the hydroxyl sites are not available for acetaldehyde adsorption, and (ii) adsorbed acetaldehyde in humid condition covers a higher surface than in dry condition. Both possibilities could be due to interactions between adsorbed acetaldehyde and water molecules. Surprisingly, the humid condition adsorption constant has been found to be 1.65 times higher than the dry condition value (Table 3). Nevertheless, due to uncertainty consideration, it is not possible to completely reject the case of equal values. However, the humid condition constant was expected to be significantly lower than the dry one.

The presented model supposes that acetaldehyde and water molecules compete for adsorption onto the same sites, but do not influence one and other. The discrepancy between the model predictions and the experimental results could be due to interactions between adsorbed acetaldehyde and water molecules. Indeed, the presented model supposes that for high acetaldehyde concentration, the surface tends to be covered by acetaldehyde

molecules and to retain no more water adsorbed molecules. In case of an interaction between adsorbed acetaldehyde and water molecules, for high acetaldehyde concentration the surface would tend to be covered with both acetaldehyde and water molecules.

3.1.4. Modeling acetaldehyde and water co-adsorption

A modified adsorption model is proposed to take into account this behavior and the above hypothesis. In this kinetic model, acetaldehyde adsorption is assumed to occur as clusters of one acetaldehyde molecule in interaction with n water molecules. Water is assumed to be adsorbed either as clusters, or as freely adsorbed molecules.

$$\begin{cases} CH_3CHO_{(g)} + nH_2O_{(g)} \rightleftarrows CH_3CHO_{(ads)}{---}nH_2O_{(ads)} \\ H_2O_{(g)} \rightleftarrows H_2O_{(ads)} \end{cases} \quad (9)$$

The adsorbed quantity of clusters is denoted by q_{CLU}. The corresponding adsorption rate is proportional to the gas-phase acetaldehyde concentration C and water vapor concentrations C_W, and to the unoccupied surface. The unoccupied surface is the difference between the water monolayer adsorbed quantity q'_m, the quantity of freely adsorbed water q_W and the number of water molecule surface occupied by one cluster. For simplification, this quantity is written as if a cluster occupied the surface on $n+1$ (for n water molecules and 1 acetaldehyde molecule) adsorbed water molecules. This assumption is not necessarily valid, but the difference can be enclosed into the value of the n constant. The cluster desorption rate is proportional to its adsorbed quantity q_{CLU}. The freely water adsorbed quantity kinetic law is also written, following the Langmuir kinetic model. Its adsorption rate is proportional to the water gas-phase concentration and to the unoccupied surface, while its desorption rate is proportional to its adsorbed quantity.

$$\begin{cases} q_{CLU} = k'_A.C.C_W[q'_m - (1+n)q_{CLU} - q_W] - k'_D.q_{CLU} \\ q_W = k_{AW}.C_W[q'_m - (1+n)q_{CLU} - q_W] - k'_{DW}.q_W \end{cases} \quad (10)$$

At equilibrium, the kinetic equations can be rewritten with the equilibrium constants $K' = \frac{k'_A}{k'_D}$ and $K_W = \frac{k_{AW}}{k_{DW}}$ to get acetaldehyde adsorption isotherm equation. It must be noticed that the adsorption and desorption constants of acetaldehyde as an acetaldehyde–water cluster are likely to be different to the acetaldehyde rate constants without water. For this reason, the adsorption constant of the cluster is written with a prime marker and is different from the adsorption constant of acetaldehyde on hydroxyl groups in dry condition, presented in Table 3.

$$q_{CLU} = \frac{q'_m.K'.C.C_W}{1 + (1+n)K'.C.C_W + K_W.C_W} \quad (11)$$

Eq. (11) can be rewritten into a Langmuir equation pattern, with apparent Langmuir model parameters $q_{m,revH}$ and K_H, which correspond to the experimentally determined ones (Table 3).

$$q_{CLU} = q_{m,revH}\frac{K_H C}{1 + K_H C} \quad (12)$$

In this equation, the acetaldehyde maximum adsorbed quantity is:

$$q_{m,revH} = \frac{q'_m}{1+n} \quad (13)$$

It can be noticed that the more water molecules acetaldehyde interacts with, the lower is the maximum adsorbed amount. Please note that q'_m is not the dry condition reversibly adsorbed maximum quantity, due to the increased hydroxylation in humid condition. However, q'_m has the same order of magnitude than the dry condition $q_{m,rev}$, the humid condition $q_{m,revH}$ is likely to be lower than the dry $q_{m,rev}$, as experimentally observed (Table 3). In Eq. (12), the apparent adsorption constant can be expressed as follow:

$$K_H = \frac{(1+n)K'.C_W}{1 + K_W.C_W} \quad (14)$$

In one hand, adsorption competition tends to make the apparent adsorption constant lower than K' (denominator of Eq. (14)). In the other hand, water–acetaldehyde interaction tends to increase the K_H value ($1+n$ factor in Eq. (14)). The fact that K' may have a different value from K must be added to these both effects. It is thus difficult to conclude about these three effects. However, K_H and K have been found to have close values. By assuming that K' and K have the same order of magnitude, it can be suggested that the adsorption competition and the interaction between acetaldehyde and water may counterbalance.

3.2. Acetic acid adsorption in dry and humid air

Similarly to acetaldehyde, acetic acid adsorption on TiO_2 is first studied in dry condition. The impact of water molecules on adsorption modes and parameters is investigated in a second step under 50% relative humidity.

3.2.1. Acetic acid adsorption in dry air: reversible and irreversible fractions

Multiple breakthrough curves and RTD of acetic acid on TiO_2 have been performed in dry condition to determine the adsorbed quantities for various acetic acid concentrations ranging from 2 to 25 ppmv. The RTD evidenced that acetic acid is adsorbed both reversibly and irreversibly in dry condition. The total adsorbed quantity did not show any significant concentration dependency. The reversible fraction is determined with the same procedure than for acetaldehyde. Fig. 7 shows the total and reversibly adsorbed quantities versus the gas phase acetic acid concentration. The total and reversibly adsorbed quantities are respectively 8.1 ± 0.6 μmol/m^2 and 0.8 ± 0.1 μmol/m^2. Similarly to the total adsorbed quantity, the reversible and irreversible fractions do not show any significant concentration dependency. It suggests that irrespectively of the input concentration, the reversibly and irreversibly adsorbed fractions always reach their maximum values. Subsequently, all the obtained adsorption equilibriums on the investigated concentration range should correspond to the TiO_2 surface saturation by acetic acid molecules, even for the lowest investigated concentrations. In the Langmuir model framework, reaching high coverage rate for such low concentrations attests a very high adsorption constant and enthalpy. Such a behavior is supposed to be incompatible with a reversible adsorption.

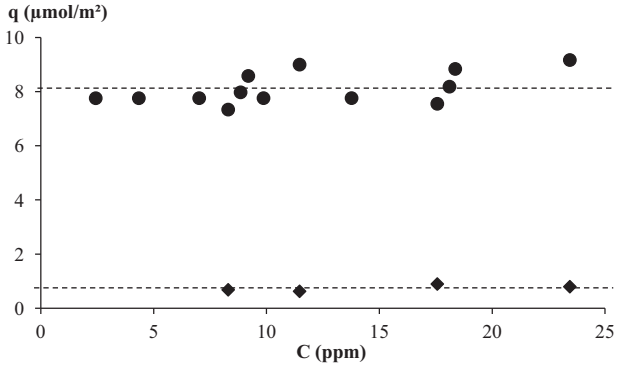

Fig. 7. Acetic acid adsorption on P25 TiO_2 isotherms under dry condition and 23 °C of total (circles) and reversibly (diamonds) adsorbed fraction.

However, a reversibly adsorbed fraction is observed for acetic acid. Nevertheless, a strong coverage dependency of the adsorption enthalpy could explain this behavior. These points, which significantly differ from acetaldehyde, are discussed more in details after the adsorption mode characterization.

3.2.2. Acetic acid adsorption modes in dry air

A TPD has been carried out to identify the adsorption modes of acetic acid on TiO_2. The TPD curve is reported in Fig. 8. It shows two peaks: an acetic acid desorption peak between 320 and 650 K, and an acetone peak above 500 K. Other species may have desorbed during the TPD, but have not been detected with the selected SIFT-MS method used. These two peaks correspond either to two adsorption modes, or to one adsorption mode desorbing under different forms, depending on the temperature.

During the TPD of acetic acid, similarly to acetaldehyde TPD, the amount of acetic acid monitored is from far lower than the irreversibly adsorbed amount. Among the acetic acid which adsorbed during the breakthrough, 9 % is desorbed during the RTD, 13% is desorbed as acetic acid, and 24% as acetone during the TPD. This behavior is due to surface reactions onto TiO_2 while heating despite the use of N_2 as carrier gas during TPD.

Regarding acetic acid adsorption on TiO_2, three modes are described in the literature: (i) dissociative chemisorption on TiO_2 as acetate groups [39,40], (ii) molecular chemisorption by Lewis acid bonding on titanium (IV) sites [40], and (iii) physisorption by hydrogen interaction on the TiO_2 surface hydroxyl groups or on other adsorbed acetic acid molecules [39,40].

To identify the adsorption modes corresponding to the observed TPD peaks, similar TPDs reported in the literature are compared with this work. Kim et al. [41,42] performed acetic acid TPD from TiO_2 anatase surface. The obtained TPD curves evidenced three desorption peaks. The first one disappeared when authors flushed the adsorption cell during sufficient time. Consequently, it is attributed to a reversible and molecular adsorption mode. During our TPD experiment, acetic acid desorption started only beyond 50 °C. Considering this threshold temperature, no reversibly adsorbed acetic acid molecules are present on TiO_2 surface anymore after flushing. The reversible adsorption can be attributed in our study to the physisorbed mode, and this mode is not present after flushing in the irreversible fraction.

The two other TPD peaks described by Kim et al. [41] are interpreted by the authors as two different desorption pathways of acetate groups: the first one produces acetic acid, while the second one mainly leads to the release of other VOCs including acetone. Several authors [41–43] evidenced that acetate groups on TiO_2 surface produce acetone while heating. The temperature range of these peaks is coherent with the observed ones on Fig. 8: from 350 to 600 K for the acetic acid peak and above 500 K for the acetone peak. The dissociative adsorption mode thus corresponds to these two peaks.

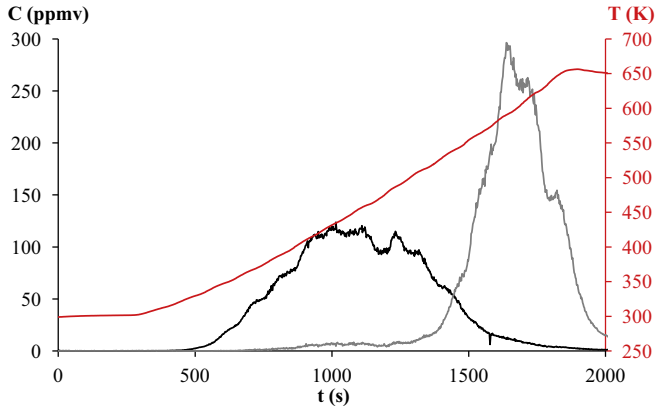

Fig. 8. Reactor outlet acetic acid (black) and acetone (grey) concentrations and reactor temperature (red) versus time during TPD of the irreversibly adsorbed acetic acid on P25 TiO_2 in dry condition, under 100 mL/min dry N_2 flow and 15 K/min heating. (For interpretation of the references to colour in this figure legend, the reader is referred to the web version of this article.)

The molecular adsorption TPD peak could be part of the acetic acid peak. Indeed, this peak covers a wide temperature range. Thus, it could correspond to two overlapped peaks of molecular and dissociative modes. A second hypothesis to explain the peak width is an important coverage dependency of the corresponding mode.

The acetic acid TPD peak has been used to estimate the adsorption enthalpy range for the adsorption mode(s) corresponding to this peak. The acetone peak cannot be used for enthalpy determination because the Langmuir model used for the calculations implies an adsorption–desorption equilibrium. In the case of acetate desorption as acetone, it cannot be ensured that acetone adsorption as acetate groups occurs during the heating. The calculation has been carried out for two different situations.

(ii) In the case of a single adsorption mode characterized by a higher coverage dependency, the enthalpies are found to range between -90 ± 21 kJ/mol ($\theta = 1$) and -114 ± 18 kJ/mol ($\theta = 0$).
(iii) The corresponding $q_{m,irr}$ value is estimated to be 1.28 ± 0.19 μmol/m^2.
(iv) In the case of two overlapped peaks corresponding to two adsorption modes, the enthalpies are found to range between -93 ± 5 kJ/mol ($\theta = 1$) and -96 ± 6 kJ/mol ($\theta = 0$) for the first mode and between -108 ± 6 kJ/mol ($\theta = 1$) and -122 ± 10 kJ/mol ($\theta = 0$) for the second mode. The corresponding $q_{m,irr}$ values are estimated to be respectively 0.62 ± 0.06 μmol/m^2 and 0.60 ± 0.05 μmol/m^2.

The one-mode hypothesis provides a better fit of the remaining adsorbed quantity curve. Moreover, the concentration curve calculated from these parameters is a wide single peak, while the curve based on the two modes rather leads to two separate thinner peaks. The large coverage-dependency could be due to electronic effects caused by the acetate-titanium chemical bounds. As a result, we can suggest that the TPD denotes a dissociative adsorption mode, leading to the release of acetic acid and acetone while heating.

3.2.3. Acetic acid adsorption in humid air

Breakthrough curves and RTD of acetic acid have been carried out to calculate the adsorbed quantities under seven different acetic acid concentrations ranging from 2 to 53 ppmv, and to assess whether acetic acid adsorption leads to reversible and irreversible fractions under 50% RH. Similarly to dry air, acetic acid adsorption has been found to be partly reversible and irreversible under humid air. Both reversible and irreversible isotherms of acetic acid on TiO_2 are displayed on Fig. 9 with their respective Langmuir model fits. The experiments have been performed three times for each concentration. The displayed data correspond to the averaged values. The fit obtained values are given in Table 4.

The irreversible adsorption of acetic acid was not expected in humid condition, since TiO_2 surface is totally hydroxylated in this condition. The presence of this fraction can only be explained by some acetic acid removing hydroxyl groups to access the titanium sites. These acetic acid molecules could come from the gas phase, but in this case the adsorption constant of both fractions would probably be more different than experimental values reported in Table 4. They can also come from the reversibly adsorbed molecules on hydroxyl groups. Reaction equilibriums between

acetic acid adsorbed as acetate groups and molecularly adsorbed acetic acid have been reported in the presence of water. Water vapor has been evidenced [39] to cause a reaction on TiO_2 surface producing chemisorbed acetate groups from physisorbed acetic acid molecules. Besides, acetate groups can react with water molecules to produce physisorbed acetic acid [40]. Consequently, acetate and H-bonded adsorption modes are in equilibrium under 50% relative humidity. A similar exchange between physically and chemically bonded modes is described in literature [37] for methanol and methoxy groups. This reaction could explain why reversible and irreversible fractions have close apparent K values. Indeed, if the irreversible adsorption occurs in two steps via the reversibly adsorbed state, only the first step will depends on the gas-phase concentration. The irreversibly and reversibly adsorbed fractions will thus share the same K value.

A model is explored to explain the observed behaviors regarding the acetic acid–acetate equilibrium.

3.2.4. Kinetic modeling of acetic acid reactive adsorption on TiO_2

A kinetic model is proposed to take surface equilibriums into account. In this model, two reactions are considered: (i) the acetic acid adsorption from gas phase onto hydroxyl groups, in competition with water molecules adsorption onto the same sites (Eq. (15)), and (ii) a chemical reaction between a physisorbed acetic acid molecule and a hydroxyl group, leading to acetate group chemisorption onto Ti (IV) atoms (Eq. (16)).

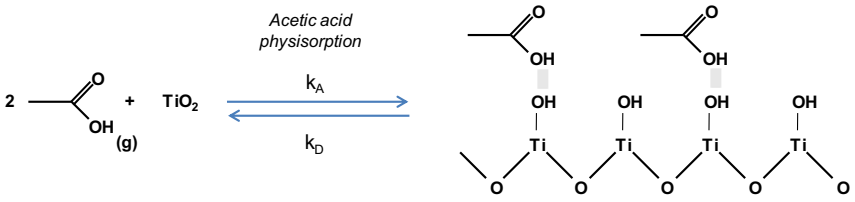

(15)

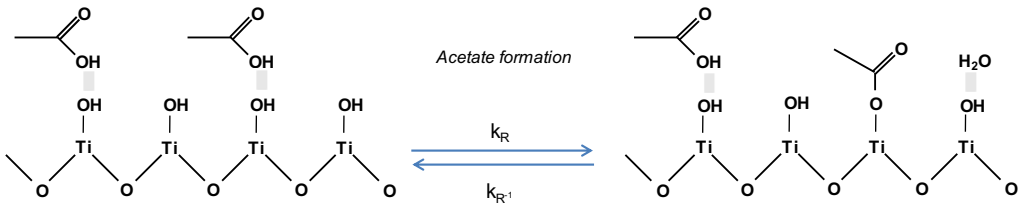

(16)

Fig. 10 gives a schematic representation of the global reactive adsorption mechanism proposed, showing that the physisorption of acetic acid molecules on TiO_2 competes with water to access –OH sites and that the dissociative adsorption is in equilibrium with the physisorbed acetic acid instead of gas phase acetic acid.

The kinetic laws of (i) physisorbed acetic acid amount (denoted by q_{rev}), (ii) acetate group quantity (denoted by q_{irr}) and (iii) adsorbed water (denoted by q_W) have first been written from the reaction pathway proposed on Fig. 10. Acetic acid and water are both adsorbed on –OH groups, their adsorption–desorption rate has been written with the competitive Langmuir model. In this model, the adsorption rate is the multiplication of a kinetic adsorption constant (respectively denoted by k_A and k_{aW} for acetic acid and water), the gas phase concentration (respectively denoted by C and C_W for acetic acid and water) and the free –OH site quantity. In order to take the adsorption competition into account, the free -OH site quantity is the number of –OH sites (denoted by q_{OH}) minus the adsorbed specie quantities: acetic acid and water. The desorption rate is the multiplication of a kinetic desorption constant (denoted by k_D and k_{DW} for acetic acid and water respectively) and the concerned compound adsorbed quantity (Eqs. (17) and (18)). The acetate production reaction from acetic acid is taken into account in the acetic acid rate law by subtracting the acetate production rate from the acetic acid adsorption rate (Eq. (17)). Acetate kinetic law is written as an acetate production rate and an acetate consumption rate. Since both reaction pathways only exist in the presence of water, a bi-molecular reaction has been assumed between water and the concerned compound (Eq. (19)).

$$\frac{dq_{rev}}{dt} = k_A.C(q_{OH} - q_{rev} - q_W) - k_D.q_{rev} - \frac{dq_{irr}}{dt} \quad (17)$$

$$\frac{dq_W}{dt} = k_{AW}.C_W(q_{OH} - q_{rev} - q_W) - k_{DW}.q_W \quad (18)$$

$$\frac{dq_{irr}}{dt} = k_R.q_W.q_{rev} - k_{R^{-1}}.q_W.q_{irr} \quad (19)$$

Once the equilibrium is reached, these three rates are equal to zero. Equilibrium constants are defined as kinetic constant ratios: $\alpha = \frac{k_R}{k_{R^{-1}}}$, $K = \frac{k_A}{k_D}$ and $K_W = \frac{k_{AW}}{k_{DW}}$. The three last equations can be written at equilibrium as:

$$q_{rev} = K.C(q_{OH} - q_{rev} - q_W) \quad (20)$$

$$q_W = K_W.C_W(q_{OH} - q_{rev} - q_W) \quad (21)$$

$$q_{irr} = \alpha\, q_{rev} \quad (22)$$

Since the surface is fully hydroxylated under 50% relative humidity, acetate group production is assumed to occur by replacing –OH groups. The hydroxyl group quantity available for acetic acid and water adsorption q_{OH} is thus the difference between the full-hydroxylation –OH group quantity q_{mOH} and the acetate group quantity q_{irr}.

$$q_{OH} = q_{mOH} - q_{irr} = q_{mOH} - \alpha\, q_{rev} \quad (23)$$

By combining the last four equations, the physisorbed acetic acid quantity can be calculated as:

$$q_{rev} = q_{mOH}\frac{K.C}{1 + (1+\alpha)K.C + K_W.C_W} \quad (24)$$

Eq. (24) can be rewritten as an effective Langmuir model equation in order to highlight the fact that this model leads to the same isotherm pattern than the Langmuir model:

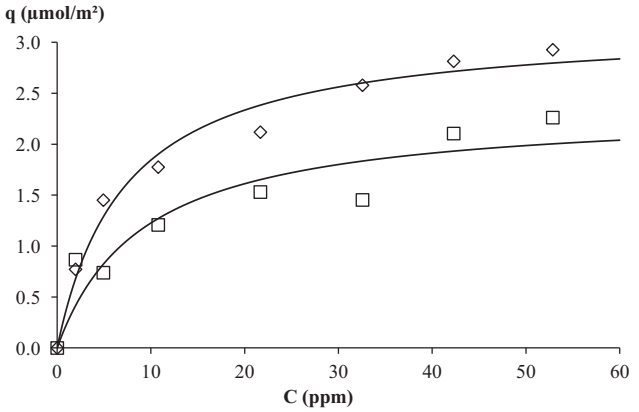

Fig. 9. Acetic acid reversibly (diamonds) and irreversibly (squares) adsorbed quantities on P25 TiO_2 isotherms under 50% RH at 23 °C, with the corresponding Langmuir model fits.

Table 4
Langmuir parameters for reversible and irreversible fractions of acetic acid adsorption on P25 TiO_2 in humid condition (50% RH), at 23 °C.

	Reversible fraction	Irreversible fraction
q_m (µmol/m^2)	3.2 ± 0.3	2.4 ± 0.1
K (ppmv^{-1})	0.14 ± 0.04	0.11 ± 0.15

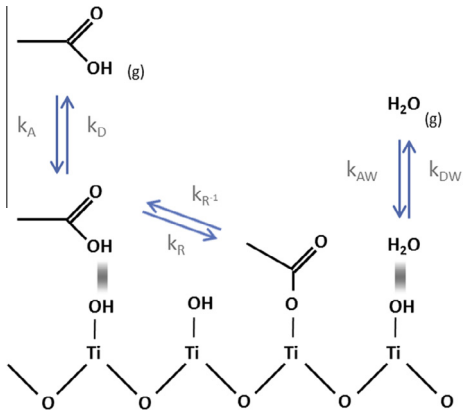

Fig. 10. Schematic representation of acetic acid adsorption modes on P25 TiO_2 under 50% RH at 23 °C.

$$q_{rev} = q_{m,revH}\frac{K_H C}{1 + K_H C} \quad (25)$$

Eq. (25) was obtained from Eq. (24) by using humid condition effective parameters:

$$q_{m,revH} = \frac{q_{mOH}}{1 + \alpha} \quad (26)$$

$$K_H = \frac{(1 + \alpha)K}{1 + K_W C_W} \quad (27)$$

This model provides two important results:

(ii) Reversible and irreversible fraction quantities are proportional, as evidenced in Eq. (22). It is consistent with the experimental values obtained for adsorption constants associated to the reversible and irreversible fractions in the humid condition which are very close.

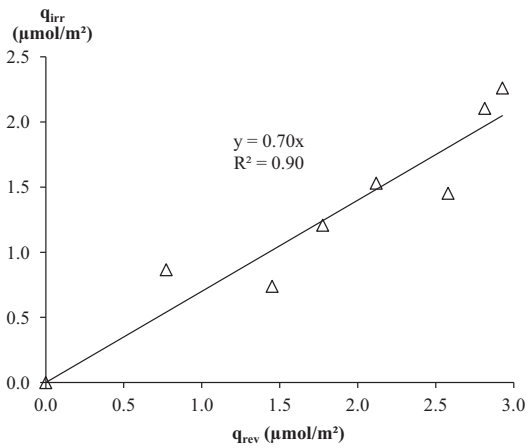

Fig. 11. Irreversibly adsorbed acetic acid quantities on P25 TiO_2 versus reversibly adsorbed acetic acid quantities under 50% RH at 23 °C.

(iii) The pseudo adsorption constant K_H is expected to be lower than the dry adsorption constant K (Eq. (27)). This is coherent with the profiled of the reversible fraction isotherms in dry (Fig. 7) and humid (Fig. 9) conditions.

The α constant can be calculated from reversibly and irreversibly adsorbed quantities. Fig. 11 reports the evolution of irreversibly adsorbed acetic acid quantities versus reversibly adsorbed quantities in humid condition. This plot confirms a linear relation between both adsorbed quantities and praises on the validity of the proposed model. Moreover, it is possible to estimate the value of α as 0.70 ± 0.49. The uncertainty on α has been calculated by taking in account q_{rev} dispersion, q_{irr} dispersion and the linear fit uncertainty.

The reversible isotherm fit using the Langmuir model provides the values of $q_{m,revH}$ and KH (Table 4) In the presence of other VOCs, competitive adsorption may occur. If the other VOCs adsorb onto hydroxyl groups, they will compete with the acetic acid reversibly adsorbed mode. The consequences of this competition on the VOCs adsorbed quantities will depend on the relative values of the apparent adsorption constant of acetic acid and other VOCs. The indirect acetic acid adsorption mode in humid condition is related to the reversibly adsorbed quantity. However, since the indirect adsorption is irreversible, its behavior in the presence of other VOCs will depend of the order of the VOC exposure.

- If acetic acid is first introduced in the system, the irreversibly adsorbed acetic acid quantity will mainly depend on the reversibly adsorbed quantity in the absence of other VOC. In this case, even if the other VOCs strongly compete with the reversibly adsorbed acetic acid, the irreversibly adsorbed fraction is not likely to be affected.
- If acetic acid is introduced after the adsorption equilibrium of other VOCs, the reversibly adsorbed acetic acid quantity is likely to be lower than in single-VOC condition, due to adsorption competition. In this case, the irreversibly adsorbed acetic acid quantity will depend on the quantity of reversibly adsorbed one and thus be lower than in single-COV condition, since the reversible fraction is affected.

In both cases, the presence of irreversibly adsorbed acetic acid will reduce the other VOC maximum adsorbed amount by decreasing the number of hydroxyl sites.

As a consequence it appears necessary to characterize the binary adsorption of acetic acid and acetaldehyde in humid

condition in order to evaluate the interaction phenomena in between these VOCs their adsorption on TiO_2.

3.3. Sequential binary adsorption of acetic acid and acetaldehyde in humid condition

Binary adsorptions of acetic acid and acetaldehyde experiments are carried out to evaluate whether it is possible to interpret multi-VOC adsorption from data obtained on single-VOC adsorption. VOCs are sequentially introduced. Indeed, the binary adsorption behavior is likely to depend on the introduction order of the VOCs, due to irreversible adsorption phenomena. The aim of this work is to get adsorption data for PCO understanding. It was thus decided to choose the VOC introduction order which mimics a PCO situation. The experiments are performed under 50% relative humidity for the same purpose. Acetic acid is likely to appear in adsorbed phase when degrading acetaldehyde. The competitive adsorption is thus studied here in the case of acetic acid introduction in the system when acetaldehyde is already at gas–solid adsorption equilibrium.

Subsequently, TiO_2 surface is first exposed to acetaldehyde, till the breakthrough (step 1), then, the surface is exposed to an acetaldehyde–acetic acid mixture (step 2) with the same acetaldehyde concentration than step 1. The acetaldehyde adsorbed quantity is calculated directly after the step 1. The acetic acid adsorbed quantity is calculated after the step 2. The acetaldehyde quantity which may desorb because of the presence of acetic acid during the step 2 is also determined. Finally the reactor is flushed with zero air (step 3) to quantify the reversibly adsorbed quantity of acetaldehyde and acetic acid in equilibrium with the VOC gas mixture.

The acetaldehyde and acetic acid quantities on the surface determined along the three different steps are reported in Table 5. For comparison, the corresponding single-VOC adsorption quantities obtained from former isotherms are given between brackets next to each quantity.

The acetaldehyde adsorption is known to be totally reversible in humid condition. The acetaldehyde quantity on the surface in presence of acetic acid is thus considered to be equal to the acetaldehyde quantity desorbing during step 3. For the same reason, a zero quantity is written for the remaining acetaldehyde quantity in step 3.

It can be noticed that the acetaldehyde quantity on the surface decreases by 88% in the presence of acetic acid. On the contrary,

Table 5
Acetaldehyde and acetic acid quantities on P25 TiO_2 surface along the three experimental steps, under 50% RH and 23 °C. Brackets: quantities in single-VOC condition, for the same concentrations, calculated with the single-VOC adsorption parameters.

VOC	Step 1: Acetaldehyde 43 ppm	Step 2: Acetaldehyde 43 ppm Acetic acid 35 ppm	Step 3: Zero air
Acetaldehyde (μmol/m^2)	0.122	0.015 (0.157 ± 0.077)	0
Acetic acid (μmol/m^2)	Ø	3.62 (4.48 ± 0.87)	1.20 (1.84 ± 0.47)

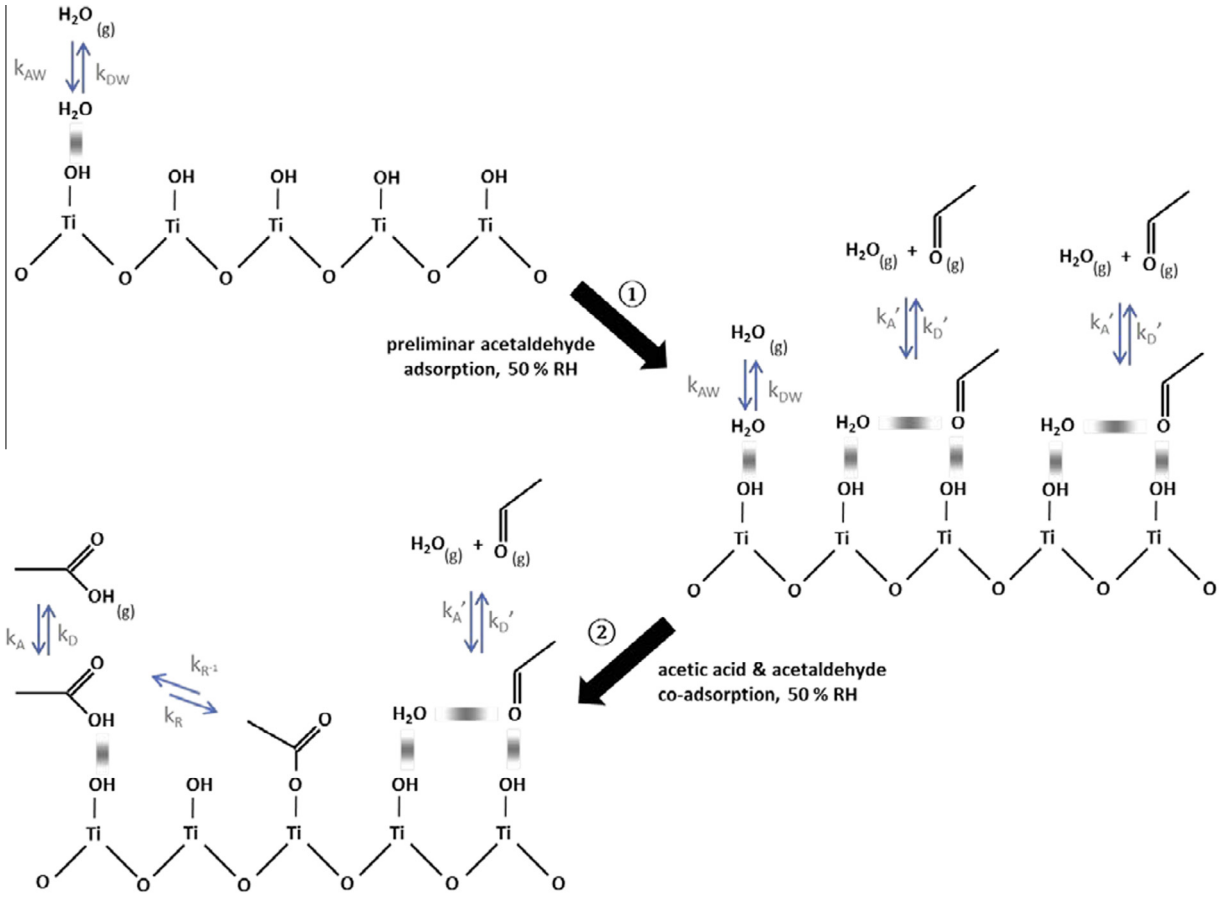

Fig. 12. Layout of ① acetaldehyde and ② subsequent acetic acid and acetaldehyde co-adsorption on P25 TiO_2 under 50% relative humidity and 23 °C.

the reversibly adsorbed acetic acid fraction is not significantly impacted by the preadsorption of acetaldehyde. This effect is due to the adsorption competition with acetic acid for adsorption onto hydroxyl groups. This adsorption competition is widely in favor of acetic acid. This result is in coherence with the adsorption apparent constants of acetaldehyde and reversibly adsorbed acetic acid in humid condition, which have a one order of magnitude difference. The same 3-step experimental sequence has been performed with 84 ppmv acetaldehyde and 31 ppmv acetic acid. It provides the same trends. Acetaldehyde adsorbed quantity decreases by 85% in presence of acetic acid. The acetic acid reversibly and irreversibly adsorbed quantities in presence of acetaldehyde are the same as in single-VOC condition.

The acetic acid irreversibly adsorbed fraction showed no significant influence on preadsorbed acetaldehyde, relatively to the uncertainties affecting these quantity values. It can thus be assumed that the presence of gaseous and physisorbed acetaldehyde do not affect the acetic acid–acetate reaction.

The observed trends for acetaldehyde and acetic acid adsorption in presence of the VOC mixture are in accordance with the qualitative and quantitative data obtained while studying individually both VOC adsorptions. These single-VOC obtained data are thus likely to be used to explain and to predict VOC adsorption in case of mixtures. These data are also likely to be used to model the kinetic of VOC mixture photocatalytic oxidation. Fig. 12 summarizes the adsorption phenomena described in humid condition during the sequential adsorption of acetaldehyde and acetic acid.

4. Conclusion

Acetaldehyde and acetic acid adsorption have been quantitatively characterized by combining breakthrough curves, room temperature desorptions and temperature-programmed desorptions. Quantitative data have been determined for the various adsorption modes of both VOCs regarding adsorbed quantities, adsorption constants and enthalpies. It first evidenced that the impact of humidity considerably differs from one VOC to another. It has been demonstrated that the various behaviors of the VOCs on TiO_2 surface are directly related to their adsorption modes and parameters, and to the VOC–water interactions in adsorbed phase. These interactions are likely to be caused by the VOC hydrophilicity. This effect could thus be correlated with the VOC solubility in water.

Since the classical Langmuir model was not able to represent (i) the influence of RH on acetaldehyde, and (ii) the reactive adsorption of acetic acid, modified models have been proposed to take these phenomena into account. The model developed for acetaldehyde and water co-adsorption raises interesting perspectives to predict the behavior of hydrophilic VOC on TiO_2 surface during photocatalytic oxidation of VOCs. Similarly, the kinetic model proposed for acetic acid reactive adsorption is a step forward in the clarification of TiO_2 massive surface coverage by carboxylic acids during photocatalytic oxidation.

Results obtained on single VOC adsorption have been useful to understand and predict the behavior of acetaldehyde and acetic acid sequential adsorption. This approach is highly informative to understand and predict the multiple VOC photocatalytic treatment. Indeed, the massive desorption of preliminarily adsorbed acetaldehyde along acetic acid co-adsorption points out the fact that adsorption considerations may explain VOC sequential treatments. Photocatalytic oxidation processes are generally observed and discussed from a global process scale, whereas the investigation of specific VOC sorption on the photocatalyst may lead to a better understanding of the oxidation reaction performance. Predictive model dedicated to photocatalytic treatment of VOC mixture have to take into account single VOC adsorption parameters.

Acknowledgments

The authors want to thank the Institut Carnot Mines for its financial support in the framework the *PhotoCair* project, and Vincent GAUDION for his valuable technical assistance.

References

[1] R. Kostiainen, Volatile organic compounds in the indoor air of normal and sick houses, Atmos. Environ. 29 (1995) 693–702, http://dx.doi.org/10.1016/1352-2310(94)00309-9.
[2] S. Schmid, M.C. Jecklin, R. Zenobi, Degradation of volatile organic compounds in a non-thermal plasma air purifier, Chemosphere 79 (2010) 124–130, http://dx.doi.org/10.1016/j.chemosphere.2010.01.049.
[3] Y.Z. Jinhan Mo, Photocatalytic purification of volatile organic compounds in indoor air: a literature review, Atmos. Environ. (2009) 2229–2246.
[4] H. Destaillats, M. Sleiman, D.P. Sullivan, C. Jacquiod, J. Sablayrolles, L. Molins, Key parameters influencing the performance of photocatalytic oxidation PCO air purification under realistic indoor conditions, Appl. Catal. B Environ. 128 (2012) 159–170, http://dx.doi.org/10.1016/j.apcatb.2012.03.014 (Heterog. Catal. Electron. Process. Photocatal. Spec. Issue Dedic. Jean-Marie Herrmann.).
[5] B. Sanchez, M. Sanchez-Munoz, M. Munoz-Vicente, G. Cobas, R. Portela, S. Suarez, et al., Photocatalytic elimination of indoor air biological and chemical pollution in realistic conditions, Chemosphere 87 (2012) 6.
[6] Y. Paz, Application of TiO_2 photocatalysis for air treatment: patents' overview, Appl. Catal. B Environ. 99 (2010) 448–460.
[7] W. Chen, J.S. Zhang, UV-PCO device for indoor VOCs removal: investigation on multiple compounds effect, Build. Environ. 43 (2008) 246–252.
[8] T.N. Obee, Photooxidation of sub-parts-per-million toluene and formaldehyde levels on titania using a glass-plate reactor, Environ. Sci. Technol. 30 (1996) 3578–3584, http://dx.doi.org/10.1021/es9602713.
[9] M.E. Zorn, S.O. Hay, M.A. Anderson, Effect of molecular functionality on the photocatalytic oxidation of gas-phase mixtures, Appl. Catal. B Environ. 99 (2010) 420–427.
[10] J.M. Coronado, M.E. Zorn, I. Tejedor-Tejedor, M.A. Anderson, Photocatalytic oxidation of ketones in the gas phase over TiO_2 thin films: a kinetic study on the influence of water vapor, Appl. Catal. B Environ. 43 (2003) 329–344, http://dx.doi.org/10.1016/S0926-3373(03)00022-5.
[11] K. Demeestere, J. Dewulf, H.V. Langenhove, B. Sercu, Gas–solid adsorption of selected volatile organic compounds on titanium dioxide Degussa P25, Chem. Eng. Sci. 58 (2003) 13.
[12] I. Sopyan, M. Watanabe, S. Murasawa, K. Hashimoto, A. Fujishima, An efficient TiO_2 thin-film photocatalyst: photocatalytic properties in gas-phase acetaldehyde degradation, J. Photochem. Photobiol. Chem. 98 (1996) 79–86.
[13] L. Zhong, C.-S. Lee, F. Haghighat, Adsorption performance of titanium dioxide (TiO_2) coated air filters for volatile organic compounds, J. Hazard. Mater. 243 (2012) 340–349, http://dx.doi.org/10.1016/j.jhazmat.2012.10.042.
[14] A.K. Boulamanti, C.J. Philippopoulos, Photocatalytic degradation of C5–C7 alkanes in the gas-phase, Atmos. Environ. 43 (2009) 3168–3174.
[15] G. Vincent, A. Queffeulou, P.M. Marquaire, O. Zahraa, Remediation of olfactory pollution by photocatalytic degradation process: study of methyl ethyl ketone (MEK), J. Photochem. Photobiol. Chem. 191 (2007) 42–50.
[16] A. Bouzaza, C. Vallet, A. Laplanche, Photocatalytic degradation of some VOCs in the gas phase using an annular flow reactor: determination of the contribution of mass transfer and chemical reaction steps in the photodegradation process, J. Photochem. Photobiol. Chem. 177 (2006) 212–217.
[17] H. Liu, Z. Lian, X. Ye, W. Shangguan, Kinetic analysis of photocatalytic oxidation of gas-phase formaldehyde over titanium dioxide, Chemosphere 60 (2005) 630–635.
[18] Y. Ohko, D.A. Tryk, K. Hashimoto, A. Fujishima, Autoxidation of acetaldehyde initiated by TiO_2 photocatalysis under weak UV illumination, J. Phys. Chem. B 102 (1998) 2699–2704, http://dx.doi.org/10.1021/jp9732524.
[19] R.M. Alberici, W.F. Jardim, Photocatalytic destruction of VOCs in the gas-phase using titanium dioxide, Appl. Catal. B Environ. 14 (1997) 55–68.
[20] V. Augugliaro, S. Coluccia, V. Loddo, L. Marchese, G. Martra, L. Palmisano, et al., Photocatalytic oxidation of gaseous toluene on anatase TiO_2 catalyst: mechanistic aspects and FT-IR investigation, Appl. Catal. B Environ. 20 (1999) 15–27.
[21] N.L. Gilbert, M. Guay, J. David Miller, S. Judek, C.C. Chan, R.E. Dales, Levels and determinants of formaldehyde, acetaldehyde, and acrolein in residential indoor air in Prince Edward Island, Canada, Environ. Res. 99 (2005) 11–17, http://dx.doi.org/10.1016/j.envres.2004.09.009.
[22] O. Debono, F. Thevenet, P. Gravejat, V. Hequet, C. Raillard, L. Lecoq, et al., Toluene photocatalytic oxidation at ppbv levels: kinetic investigation and carbon balance determination, Appl. Catal. B Environ. 106 (2011) 600–608.
[23] O. Debono, F. Thévenet, P. Gravejat, V. Héquet, C. Raillard, L. Le Coq, et al., Gas phase photocatalytic oxidation of decane at ppb levels: removal kinetics, reaction intermediates and carbon mass balance, J. Photochem. Photobiol. Chem. 258 (2013) 17–29, http://dx.doi.org/10.1016/j.jphotochem.2013.02.022.
[24] D. Farhanian, F. Haghighat, Photocatalytic oxidation air cleaner: identification and quantification of by-products, Build. Environ. 72 (2014) 34–43, http://dx.doi.org/10.1016/j.buildenv.2013.10.014.

[25] W. Chan, S.-C. Lee, Y. Chen, B. Mak, K. Wong, C.-S. Chan, et al., Indoor air quality in new hotels' guest rooms of the major world factory region, Int. J. Hosp. Manage. 28 (2009) 26–32.
[26] I. Langmuir, The adsorption of gases on plane surfaces of glass, mica and platinum, J. Am. Chem. Soc. (1918) 1361–1403.
[27] A. Bourane, O. Dulaurent, K. Chandes, D. Bianchi, Heats of adsorption of the linear CO species on a Pt/Al2O3 catalyst using FTIR spectroscopy: comparison between TPD and adsorption equilibrium procedures, Appl. Catal. Gen. 214 (2001) 193–202.
[28] E.A. Redekop, G.S. Yablonsky, D. Constales, P.A. Ramachandran, C. Pherigo, J.T. Gleaves, The Y-procedure methodology for the interpretation of transient kinetic data: analysis of irreversible adsorption, Chem. Eng. Sci. 66 (2011) 6441–6452, http://dx.doi.org/10.1016/j.ces.2011.08.055 (Nov. Gas Convers. Symp.- Lyon 2010 C1-C4 Catal. Process. Prod. Chem. Fuels).
[29] R.J. Cvetanović, Y. Amenomiya, Application of a temperature-programmed desorption technique to catalyst studies, in: H. Pines, P.B. Weisz, D.D. Eley (Eds.), Advances in Catalysis, Academic Press, 1967, pp. 103–149 (<http://www.sciencedirect.com/science/article/pii/S0360056408606860>).
[30] P.A. Redhead, Thermal desorption of gases, Vacuum 12 (1962) 203–211, http://dx.doi.org/10.1016/0042-207X(62)90978-8.
[31] J.M. Kanervo, T.J. Keskitalo, R.I. Slioor, A.O.I. Krause, Temperature-programmed desorption as a tool to extract quantitative kinetic or energetic information for porous catalysts, J. Catal. 238 (2006) 382–393.
[32] M. Singh, N. Zhou, D.K. Paul, K.J. Klabunde, IR spectral evidence of aldol condensation: acetaldehyde adsorption over TiO_2 surface, J. Catal. 260 (2008) 371–379.
[33] J. Rasko, J. Kiss, Adsorption and surface reactions of acetaldehyde on TiO_2, CeO_2 and Al_2O_3, Appl. Catal. Gen. 287 (2005) 252–260.
[34] Z. Topalian, B.I. Stefanov, C.G. Granqvist, L. Österlund, Adsorption and photo-oxidation of acetaldehyde on TiO_2 and sulfate-modified TiO_2: studies by in situ FTIR spectroscopy and micro-kinetic modeling, J. Catal. 307 (2013) 265–274, http://dx.doi.org/10.1016/j.jcat.2013.08.004.
[35] B.I. Stefanov, Z. Topalian, C.G. Granqvist, L. Österlund, Acetaldehyde adsorption and condensation on anatase TiO_2: influence of acetaldehyde dimerization, J. Mol. Catal. Chem. 381 (2014) 77–88, http://dx.doi.org/10.1016/j.molcata.2013.10.005.
[36] M. Nagao, Y. Suda, Adsorption of benzene, toluene, and chlorobenzene on titanium dioxide, Langmuir (1989) 42–47.
[37] C. Wang, H. Groenzin, M.J. Shultz, Comparative study of acetic acid, methanol, and water adsorbed on anatase TiO_2 probed by sum frequency generation spectroscopy, J. Am. Chem. Soc. 127 (2005) 9736–9744, http://dx.doi.org/10.1021/ja051996m.
[38] L. Sivachandiran, F. Thevenet, P. Gravejat, A. Rousseau, Isopropanol saturated TiO_2 surface regeneration by non-thermal plasma: influence of air relative humidity, Chem. Eng. J. 214 (2013) 17–26, http://dx.doi.org/10.1016/j.cej.2012.10.022.
[39] M.J. Backes, A.C. Lukaski, D.S. Muggli, Active sites and effects of H_2O and temperature on the photocatalytic oxidation of ^{13}C-acetic acid on TiO_2, Appl. Catal. B Environ. 61 (2005) 21–35, http://dx.doi.org/10.1016/j.apcatb.2005.03.012.
[40] L.-F. Liao, C.-F. Lien, J.-L. Lin, FTIR study of adsorption and photoreactions of acetic acid on TiO_2, Phys. Chem. Chem. Phys. 3 (2001) 3831–3837.
[41] K.S. Kim, M.A. Barteau, Pathways for carboxylic acid decomposition on TiO_2, Langmuir 4 (1988) 945–953.
[42] K.S. Kim, M.A. Barteau, Structure and composition requirements for deoxygenation, dehydration, and ketonization reactions of carboxylic acids on TiO_2(001) single-crystal surfaces, J. Catal. 125 (1990) 353–375.
[43] M.A. Hasan, M.I. Zaki, L. Pasupulety, Oxide-catalyzed conversion of acetic acid into acetone: an FTIR spectroscopic investigation, Appl. Catal. Gen. 243 (2003) 81–92, http://dx.doi.org/10.1016/S0926-860X(02)00539-2.